The uptake of hydroxypropyl methacrylamide based homo, random and block copolymers by human multi-drug resistant breast adenocarcinoma cells

Matthias Barz[1,#], **Robert Luxenhofer**[2,#,†], **Rudolf Zentel**[1], and **Alexander V. Kabanov**[2]

[1]Institute of Organic Chemistry, Johannes Gutenberg-University Mainz, Duesbergweg 10-14, 55099 Mainz, Germany

[2]Department of Pharmaceutical Sciences and Center for Drug Delivery and Nanomedicine, College of Pharmacy, University of Nebraska Medical Center, Omaha, Nebraska 68198-5830, USA

Abstract

A series of well defined, fluorescently labelled homopolymers, random and block copolymers based on N-(2-hydroxypropyl)-methacrylamide was prepared by reversible addition-fragmentation chain transfer polymerization (RAFT-polymerization). The polydispersity indexes for all polymers were in the range of 1.2 to 1.3 and the number average of the molar mass (M_n) for each polymer was set to be in the range of 15 kDa to 30 kDa. The cellular uptake of these polymers was investigated in the human multi-drug resistant breast adenocarcinoma cell line MCF7/ADR. The uptake greatly depended on the polymer molecular mass and structure. Specifically, smaller polymers (approx. 15 kDa) were taken up by the cells at much lower concentrations than larger polymers (approx. 30 kDa). Furthermore, for polymers of the same molar mass, the random copolymers were more easily internalized in cells than block copolymers or homopolymers. This is attributed to the fact that random copolymers form micelle-like aggregates by intra- and interchain interactions, which are smaller and less stable than the block copolymer structures in which the hydrophobic domain is buried and thus prevented from unspecific interaction with the cell membrane. Our findings underline the need for highly defined polymeric carriers and excipients for future applications in the field of nanomedicine.

Introduction

The last decades have seen a steady increase of interest in polymer therapeutics and nanomedicines[1] such as conjugates of drugs or proteins with synthetic polymers as well as drugs incorporated in dendrimers, polymeric micelles or vesicles of different structure.[1-5] Various systems have reached clinical trials and some have been approved for the human use.[6-14]

It is widely recognized that the interactions of nanomaterials with cells define the toxicity, endocytosis and intracellular localization of such materials and altogether are critically important for the material performance in drug delivery. Studies by numerous groups found that the cellular interactions of nanomaterials in the absence of ligands for specific receptors can be affected by virtually any aspect of the nanomaterial structure and chemistry. In

CORRESPONDING AUTHOR FOOTNOTE: Prof. Dr. A. V. Kabanov, Tel Tel: (402) 559-9364, Fax: (402) 559-9365, akabanov@unmc.edu; Prof. Dr. R. Zentel, Tel: +49-6131-39-20361, Fax: +49-6131-39-24778, zentel@uni-mainz.de.
#Both authors have equally contributed
†**Current Address:** Professur für Makromolekulare Chemie, Department Chemie, TU Dresden, 01062 Dresden, Germany

particular, the cellular uptake and even route of endocytosis of various polymers and nanoparticles depend on their size[15], architecture[16], surface charge[17], charge density [18], surface structure[18], and hydrophilic-lipophilic balance.[19] For the members of the family of poly(ethylene oxide)-poly(propylene oxide)-poly(ethylene oxide) amphiphilic triblock copolymers (Pluronic) the structural effects on the interaction with cell membranes have been investigated in great detail. Recently Sahay et al. reported that the uptake route of Pluronic P85 switches from caveolae mediated endocytosis to uptake through clathrin coated pits when the concentration of the copolymer is increased from below to above the critical micelle concentration (cmc).[20] Another material of considerable interest in the nanomedicine and drug delivery fields is poly(*N*-(2-hydroxypropyl) methacrylamide) (pHPMA), which has been extensively used in polymer-drug conjugates and various block copolymer-based systems.[21-24] In this study we investigate the differences in cellular uptake between the aggregate forming HPMA-based amphiphilic block copolymers and random copolymers having the same monomer composition but different polymer architecture. Such structure-property relationships could only be reasonably obtained with polymers that are structurally and chemically well defined. HPMA is typically polymerized by free radical polymerization with functional comonomers. However, this method results in a broad molar mass distribution of the copolymer, and is further complicated by a dependence of the copolymer composition on the conversion of the reaction, which is observed when reactivities of different monomers are not perfectly matched. Furthermore, the precise molar mass determination of amphiphilic copolymers by gel permeation chromatography (GPC) or nuclear magnetic resonance (NMR) is often complicated by the aggregation of these copolymers in solution.[25-27] Recent advances in controlled radical polymerization techniques including the atom transfer radical (ATRP) polymerization[28-30] and the reversible addition-fragmentation chain transfer (RAFT) polymerization[31-33] can produce well defined polymers. Using these techniques it is possible to synthesize random copolymers as well as block copolymers. Furthermore, functional polymers can also be synthesized by these methods using functional monomers such as active esters established by Ringsdorf et al.[34-37] This synthetic pathway has two main advantages. First, it can produce random copolymers by polymer-analogue transformation of precisely characterized functional homopolymer precursors. Second, amphiphilic block copolymers can be produced from functional precursors, which consist only of hydrophobic blocks and can be precisely characterized by GPC in solvents such as tetrahydrofuran, dioxane or hexafluoroisopropanol.

Here, we employ RAFT polymerization to produce defined HPMA homopolymers as well as random and block copolymers of HPMA and laurylmethacrylate of comparable molar mass. By this approach it was possible to compare the cellular uptake of various polymer architectures based on identical monomers. In the following article we invastigate the influence of molar mass and polymer architecture on the endocytosis of the HPMA-based polymers in the multi-drug resistant (MDR) breast cancer cell line MCF7/ADR. This study underscores a need for highly defined polymers for applications in the field of nanomedicine.

Experimental Section

2.1 Materials.

All chemicals were reagent grade and obtained from Aldrich. The chemicals were used without further purification unless otherwise indicated. The Oregon green 488 cadaverine was obtained from Invitrogen. Dioxane used in the synthesis was freshly distilled from a sodium/potassium mixture. 2,2′-Azobis(isobutyronitrile) (AIBN) was recrystallized from diethyl ether and stored at −7°C. Lauryl methacrylate was distilled and kept at −7°C.

2.2 Characterization.

^{1}H-, ^{13}C- and ^{19}F-NMR spectra were obtained at 300 or 400 MHz using a FT-spectrometer from Bruker and analyzed using the ACDLabs 6.0 software. The polymers were dried at 40 °C over night under vacuum and afterwards submitted to gel permeation chromatography (GPC). GPC was performed in tetrahydrofurane (THF) as solvent and with following parts: pump PU 1580, auto sampler AS 1555, UV-detector UV 1575, RI-detector RI 1530 from Jasco and miniDAWN Tristar light scattering detector from Wyatt. Columns were used from MZ-Analysentechnik: MZ-Gel SDplus 10^2 Å, MZ-Gel SDplus 10^4 Å and MZ-Gel SDplus 10^6 Å. The elution diagrams were analysed using the ASTRA 4.73.04 software from Wyatt Technology. Calibration was done using polystyrene standards. The flow rate was 1 mL/min at a temperature of 25 °C.

2.3 Synthesis of 4-cyano-4-((thiobenzoyl)sulfanyl)pentanoic acid.

The 4-cyano-4-((thiobenzoyl) sulfanyl)pentanoic acid was used as the CTA and synthesized according to the literature.[32]

2.4 Synthesis of pentafluoro-phenyl methacrylate (PFMA).

PFMA was prepared according to the literature.[36]

2.5 General synthesis of the macro-CTA.

The macro-CTA was prepared according to the literature.[37] The RAFT polymerizations of the PFMA using 4-cyano-4-((thiobenzoyl) sulfanyl) pentanoic acid were performed in a schlenk tube. The reaction vessel was loaded with 2,2′-azobis(isobutyronitrile (AIBN), 4-cyano-4-((thiobenzoyl)sulfanyl)pentanoic acid (CTA) (molar ratio of AIBN/CTA = 1:8) and 15 g of PFMA in 20 mL of dioxane. Following three freeze–vaccum–thaw cycles, the tube was immersed in an oil bath at 70 °C. Afterwards the polymer poly(PFMA) was 3 times precipitated into hexane, isolated by centrifugation and dried for 12 hours at 30 °C under vacuum. In the end a slightly red powder was obtained. Yield: (59 %). ^{1}H NMR (CDCl$_3$): 1.6-2.2 (br), 0.9-1.5 (br) δ [ppm] ^{19}F NMR (CDCl$_3$): δ [ppm] −165.0 (br), −159.7 (br), −153.1 (br)

2.5 General synthesis of the random copolymers.

The RAFT polymerizations of the PFMA using CTA were performed in a schlenk tube. The reaction vessel was loaded with AIBN, CTA (molar ratio of AIBN/CTA = 1:8) and 15 g of PFMA in 20 mL of dioxane. Following three freeze-vaccum-thaw cycles, the tube was immersed in an oil bath at 70 °C. Afterwards the polymer poly(PFMA) was 3 times precipitated into hexane, isolated by centrifugation and dried for 12 hours at 30 °C under vacuum. In the end a slightly red powder was obtained. Yield: (67 %). ^{1}H NMR (CDCl$_3$): δ [ppm] 1.6-2.2 (br), 0.9-1.5 (br), 0.8-0.9 (br t) ^{19}F NMR (CDCl$_3$): δ [ppm] −165.1 (br), −159.6 (br), −153.2 (br)

2.7 General synthesis of block copolymers.

The block copolymer was prepared according to the literature.[26] The macro CTA obtained in the above-mentioned polymerization was dissolved in dioxane and AIBN was added. Nitrogen was bubbled through the solution and three freeze-vacuum-thaw cycles were applied. Afterwards the tube was immersed in an oil bath at 70 °C. After polymerization time of 12 h, the solution was slightly concentrated and precipitated twice in ethanol and diethyl ether, removed by centrifugation, and dried overnight at 30 °C in vacuum. A slightly red powder was obtained. Yield: (89 %). ^{1}H NMR (CDCl$_3$): δ [ppm] 1.6-2.2 (br), 0.9-1.5 (br), 0.8-0.9 (br t) ^{19}F NMR (CDCl$_3$): δ [ppm] −165.2 (br), −159.8 (br), −153.4 (br)

2.8 Removal of dithioester endgroups.

The dithiobenzoate end group was removed according to the procedure reported by Perrier et al..[38] Typically 200 mg of polymer, (Mn = 25.000 g/mol), and 50 mg of AIBN (30 times excess in relation to the polymer endgroup) were dissolved in 3 mL of anhydrous dioxane/DMSO (4:1). The solution was heated at 80 °C for 2 h. Finally the copolymer was precipitated 3 times in 100 mL of diethyl ether and collected by centrifugation. In the case of the block copolymer the crude product was first precipitated in EtOH 2 times and than 1 time in diethyl ether. The copolymer was dried under vacuum for a period of 24 h and a colourless product was obtained (yield: 92 %). The absence of the dithiobenzoate end group was confirmed by UV-Vis spectroscopy.

2.9 Polymer analogous reactions of homopolymers.

In a typical reaction 300 mg of PPFMA without ditihioester endgroup were dissolved in 4 mL abs. dioxane and 1 mL abs. DMSO. A colorless solution was obtained. In a typical reaction 2.5 mg for the 50000 g/mol precursor and 5 mg for the 25000 g/mol precursor of Oregon green 488 cadaverine and 20 mg of triethylamine were added. The mixture was kept at 25 °C for 4 h and finally 200 mg of hydroxypropylamine and 200 mg triethylamine were added. The reaction was allowed to proceed under the above mentioned conditions over night. The solution was concentrated in vacuum and introduced to a column filtration using Sephadex™ LH-20 in dioxane and precipitated in diethyl ether, removed by centrifugation and dried in vacuum at 30 °C for 14 hours. Yield: (86 %). ^{1}H NMR (DMSO-d6): δ [ppm] 3.4-3.9 (br), 2.6-3.0, 0.9-1.5 (br)

2.10 Polymer analogous reactions of random copolymers.

In a typical reaction 300 mg of PPFMA without ditihioester endgroup were dissolved in 4 mL abs. dioxane and 1 mL abs. DMSO. A colorless solution was obtained. In a typical reaction 2.5 mg for the 50000 g/mol precursor and 5 mg for the 25000 g/mol precursor of Oregon green 488 cadaverine and 20 mg of triethylamine were added. The mixture was kept at 25 °C for 4 hours and finally 200 mg of hydroxypropylamine and 200 mg triethylamine were added. The reaction was allowed to proceed under the above mentioned conditions over night. The solution was concentrated in vacuum and introduced to a column filtration using Sephadex™ LH-20 in dioxane and precipitated in diethyl ether, removed by centrifugation and dried in vacuum at 30 °C for 14 hours. Yield: (79 %). ^{1}H NMR (DMSO-d6): δ [ppm] 3.4-3.9 (br), 2.6-3.0 (br), 0.9-1.5 (br), 0.8-0.9 (br t)

2.11 Polymer analogous reactions of block copolymers.

In a typical reaction 300 mg of poly(PFMA)-block-poly(lauryl methacrylate) were dissolved in 4 ml abs. dioxane and 1 ml abs. DMSO. A colourless solution was obtained. In a typical reaction 5 mg of Oregon green 488 cadaverin and 20 mg of triethylamine were added. The mixture was kept at 25 °C for 4 hours. In the end 200 mg of hydroxypropylamine and 200 mg triethylamine were added. The reaction was allowed to go on under the above mentioned conditions over night. The solution was concentrated in vacuum and introduced to a column filtration using Sephadex™ LH-20 in dioxane/DMSO (4:1) and precipitated in diethyl ether, removed by centrifugation and dried in vacuum at 30 °C for 14 hours. Yield: (81%). ^{1}H NMR (DMSO-d6): δ [ppm] 3.4-3.9 (br), 2.6-3.0 (br), 0.9-1.5 (br), 0.8-0.9 (br t)

2.12 Characterization in Solution.

The aqueous solutions were prepared using Millipore water (deionized water, resistance >18 MΩ) and abs. DMSO. Pyrene (Aldrich, 98%) was used as fluorescent probe without further purification.

2.13. Pyrene Fluorescence Spectroscopy.[39-41]

A stock solution of each block copolymer was prepared at a concentration of 0.1 g/L by dissolving the polymer in DMSO. The polymer stock solution was then diluted to 10 different concentrations down to 1×10^{-6} g/L using an aqueous NaCl solution. Each sample was then prepared by dropping carefully 40 μL of a pyrene solution (2.5×10^{-5} mol/L in acetone) into an empty vial, evaporating the acetone by gentle heating at 50-60 °C, adding 2 mL of one of the polymer solutions, and stirring the closed and light-protected vials 48-72 h at 50-60 °C. The final concentration of pyrene in water thus reached 5.0×10^{-7} mol/L, which is slightly below the pyrene saturation concentration in water at 22 °C. Steady-state fluorescence spectra of the air-equilibrated samples were recorded using a Perkin Elmer Luminescence Spectrometer LS 50 B spectrofluorophotometer (right angle geometry, 1 cm × 1 cm quartz cell) using the following conditions: excitation at 333 nm, slit width 10 nm for the excitation, and 2.5 nm for the emission. The intensities of the bands I1 at 372 nm and I3 at 383 nm were then evaluated, and their ratio was plotted vs the polymer concentration.

2.14. Light scattering experiments of Nanoaggregates.

A total of 10 mg of the poly(HPMA)-*block*-poly(lauryl methacrylate) polymer were dissolved overnight in 10 mL of 1×10^{-3} M solution of lithium trifluoroacetate in hexafluorisopropanol (HFIP). The solution was filtered with an anatop 20 nm filter. A total of 40 mg of the block copolymer solution (*c*) 1 mg/ml) were added drop wise to 2.2×10^{-3} mg of an aqueous solution of sodium bromide (NaBr; $1 \times 10\text{-}3$ M). Under this condition, the influence of the solvent (HFIP) can be disregarded. The aggregates were analyzed right after the preparation by dynamic light scattering. For dynamic light scattering (DLS), an ALV-SP125 goniometer, an ALV-5000 correlator, a Spectra Physics 2060 Argon ion laser (500 mW output power at λ) 514.5 nm wavelength) were utilized. The scattered intensity was divided by a beam splitter (approximately 50:50), each portion of which was detected by a photomultiplier. The two signals were cross-correlated to eliminate nonrandom electronic noise. The complex solutions were typically measured from 30-150° in steps of 10° (DLS). The correlation functions showed a monomodal decay and were fitted by a sum of two exponentials, from which the first cumulant Γ was calculated. The *z*-average diffusion coefficient D_z was obtained by extrapolation of $\Gamma/q2$ to $q = 0$, leading to the inverse *z*-average hydrodynamic radius $R_\text{h} = \langle R_\text{h}^{-1} \rangle_z^{-1}$ by formal application of Stokes law.

2.14. Cell culture.

MCF7-ADR cells (derived from human breast carcinoma cell line, MCF7 (ATCC HT-B22) by selection with Doxorubicin, was kindly presented by Y.L. Lee (William Beaumont Hospital, Royal Oak, MI) and were maintained in Dulbecco's Modified Eagle's Medium (DMEM), containing 10% heat inactivated fetal bovine serum (FBS) and 1% penicillin/ streptomycin as described elsewhere.[46] All tissue material media was obtained from Gibco Life Technologies, Inc. (Grand Island, NY). Cells were used 2 days after plated unless otherwise stated.

2.15. Evaluation of cytotoxicity of Polymers; MTT assay.

MCF7/ADR were seeded in 96 well plates (10^4 cells per well) and were allowed to reattach for 24 h. Treatment solutions were prepared from a 1 mg/mL polymer stock solution in assay buffer (containing 122 mM NaCl, 25 mM NaHCO$_3$, 10 mM glucose, 10 mM HEPES, 3 mM KCl, 1.2 mM MgSO$_4$, 1.4 mM CaCl$_2$, and 0.4 mM K$_2$HPO$_4$, pH 7.4) by appropriate dilution with media (Dulbecco's Modified Eagle's Medium (DMEM), supplemented with 10% fetal bovine serum (FBS), 25 mM HEPES and penicillin/streptomycin). The cells were incubated for 48 h with 200 μL of treatment solution. After discarding the treatment solution, cells were washed thrice with PBS. FBS-free DMEM (100 μL/well) as well as 25

µL of a 5 mg/mL solution of 3-(4,5-dimethylthiazol-2-yl)-2,5-diphenyltetrazolium bromide (MTT, Invitrogen, Eugene, Oregon) in PBS were added and the cells incubated at 37 °C for 2 hours. The media was discarded subsequently and replaced with 100 µL of solvent (25% v/v DMF, 20% w/v SDS in H2O). The purple formazan product was allowed to dissolve over night and the absorbance at 570 nm was obtained using a plate reader (SpectraMax M5, Molecular Devices). Positive control cells were treated with media alone, negative controls were wells without cells. Each concentration was repeated in four wells, results are expressed as mean ± SEM.

2.16. Flow cytometry.

For the analysis of cellular uptake by flow cytometry, MCF7/ADR cells were plated in 24 well plates (7.5×10^4 per well) two days prior to the experiment. Cells were treated with 200 µL of polymer solutions in FBS free media or assay buffer. In the case of experiment performed at 4 °C, the cells were pre-washed 3 times with ice cold PBS and incubated with ice-cold polymer solution. Cells were incubated for 60 min or the indicated time at 37 °C/ 5% CO_2 or 4°C, washed subsequently thrice with ice-cold PBS, trypsinized and centrifuged. The cell pellet was resuspended in 400 µL PBS with 1% bovine serum albumin, split in two aliquots and analyzed using flow cytometry. Each data point was performed in triplicate. The mean fluorescence intensity was analyzed using Becton Dickinson FACStarPlus flow cytometer operating under Lysis II (San Jose, CA) equipped with an argon ion laser. Data were acquired in linear mode and visualized in logarithmic mode. Approximately 10,000 digital list mode events were collected and the data gated on forward and side scatter parameters to exclude debris and dead cells. Control cells without labelled polymers were used as the negative control for autofluorescence. Data analysis was performed using DiVa software.

2.17. Confocal fluorescence microscopy.

For live cell confocal microscopy (Carl Zeiss LSM 510 Meta, Peabody, MA) MCF7/ADR cells (4×10^4) were plated in Lab-Tek Chambered Cover Glasses dishes (Fischer Scientific, Waltham, MA) and after two days (37 °C, 5% CO_2) were exposed for 60 min to Oregon green labelled polymer solutions in FBS free media. Subsequently, cells were washed (3x PBS) and kept in complete media for imaging using the confocal microscope.

Results and Discussion

In order to investigate the influence of polymer architecture on the cellular uptake we synthesized by RAFT polymerization a series of fluorescently labelled HPMA-based homopolymers, random copolymers and block copolymers of different molar mass. The synthesis reactions are shown in Scheme 1.

First, the active ester polymer precursors **P1R** to **P6R** were synthesized using an approach proposed by Ringsdorf group.[34-37] Second, these functional precursors were transformed by aminolysis into final HPMA based polymers **P1** to **P6**.

Second, these functional precursors were transformed by aminolysis into final HPMA based polymers **P1** to **P6**. To obtain fluorescently labelled polymers the reactive precursor polymers were aminolysed in the presence of Oregon green 488 cadaverin and 2-hydroxy isopropan-1-ol. In average each polymer chain was labelled with one molecule of dye. For all polymer samples the conversion of the pentafluorophenyl-derivative to the HPMA was full as determined by a complete disappearance of the ^{19}F signal in the ^{19}F NMR spectra of the final polymers. Due to the use of dithiobenzoate derivatives as chain transfer agents (CTA) the end groups of the synthesized polymers represented a dithiobenzoic ester, which

can undergo side reactions during the aminolysis of the pentafluorophenyl ester.[38] In order to avoid these side reactions the end group was removed prior to the aminolysis by large excess of AIBN.

For each polymer architecture two samples with different molar mass were synthesized. The molar masses and polydispersity indexes (PDI) of the precursor polymers **P1R** to **P6R** were determined by GPC. The molar mass and PDI of the precursors and final polymers are listed in Tables 1 and 2, respectively.

The molar masses of the homopolymers were in the range established for clinically investigated pHPMA-based drug conjugates like PK1 and PK2.[3] The PDI values suggested that these polymers had relatively narrow molar mass distribution, which is characteristic of polymers synthesized by RAFT polymerization (PDI 1.1-1.3).[31] The random copolymers and block copolymers had comparable molar masses and PDI. However, due to their architecture the block copolymers formed micelle-like aggregates in aqueous solutions. These aggregates were spherical and had sizes ranging from about 100 nm to about 200 nm as determined by dynamic and static light scattering as well as by cryo transmission electron microscopy (cryo TEM) imaging experiments.[26]

To verify the concentration-dependent aggregation of the block copolymers **P5** and **P6** and determine the cmc the pyrene fluorescence technique was applied.[39-41] Pyrene has a very low solubility in water and upon formation of the micelles transfers preferentially into their hydrophobic cores. This is accompanied by a red shift in the pyrene fluorescence spectrum and changes in relative peak intensities of the spectrum's vibrational fine structure.[41] To determine the onset of the micelle formation we analysed the pyrene emission spectra asreported previously by Müller et al.[39] as well as by Winnik[40] and co workers. Figure 1 shows the dependencies of the intensity ratio I1/I3 vs. concentration of polymer in aqueous solution at pH 7.

The I1/I3 values remained constant (~1.7-1.8) at the polymer concentrations $c < 6.0 \times 10^{-5}$ mg/mL ($c < 4.8 \times 10^{-9}$ mol/L) for **P5** and $c < 5.5 \times 10^{-6}$ mg/mL ($c < 2.0 \times 10^{-10}$ mol/L) for **P6**. These I1/I3 values suggest that in the corresponding ranges of the copolymer concentrations pyrene was in aqueous environment and the micelles did not form. At higher concentrations the I1/I3 decreased suggesting that the micelles were formed and pyrene transferred into the hydrophobic environment. The cmc values (Table 3) were determined as the intersections between the plateau at I1/I3 ~ 1.7-1.8 and the tangent of the decrease of I1/I3 vs. concentration in Figure 1. These values for the block copolymers **P5** and **P6** are rather low, which is attributed to the presence of highly hydrophobic lauryl methacrylate side chains in the hydrophobic blocks. Furthermore the cmc, of **P6** is lower than that of **P5**, which is consistent with the larger hydrophobic block in **P6**.

Interestingly, the random copolymers **P3** and **P4** also exhibited a cmc-like behaviour. Specifically, the I1/I3 values for these copolymers decreased above certain concentrations. This suggested aggregation of the copolymers and formation of hydrophobic domains, in which pyrene was incorporated. However, the concentrations corresponding to the onset of the I1/I3 decrease, which for simplicity we will also call "cmc", were considerably higher than the cmc values for **P5** and **P6**. Furthermore, the sizes of the aggregates of **P3** and **P4** determined by dynamic light scattering practically did not depend on the copolymer molecular masses, while the sizes of the **P5** and **P6** micelles increased as the copolymer mass increased (Table 4).

Previous work suggests that the aggregates of the amphiphilic random copolymers in selective solvents are essentially indistinguishable from micelles.[42-45] Such aggregates in aqueous dispersions often consist of dense hydrophobic cores surrounded by a corona of

swollen loops formed by the hydrophilic parts of the polymer (Figure 2). The formation of the loops leads also to smaller hydrophilic corona as well as less defined and less stable aggregates, which in case of **P3** and **P4** is reflected in a slightly higher μ_2 value and higher cmc. Furthermore a certain number of accessible lauryl side chains in the hydrophilic loop can be expected, because a complete separation of hydrophilic and hydrophobic parts will be precluded by steric hindrance and unfavorable entropy term.

The HPMA homopolymer is well known to be non-toxic and non-immunogenic. Recently we reported that HPMA-lauryl methacrylate block copolymers are also non-toxic to MDCKII cells in concentrations of up to 2 mg/mL.[26] However, we could not exclude that random copolymers were toxic and, therefore, evaluated the cell toxicity of all polymers in MDR breast adenocarcinoma cell line MCF7/ADR using standard 3-(4,5-dimethylthiazol-2-yl)-2,5-diphenyltetrazolium bromide (MTT) assay. Since we observed no decrease in cell viability following exposure of the cells for 48 h to the random copolymers at concentrations of up to 0.1 mg/mL we concluded that they were safe up to this dose. Next, we investigated the cellular uptake of the fluorescently labelled polymers by flow cytometry. For this purpose the adherent MCF7/ADR cells in 24-well plates were exposed for 60 min to polymer solutions at concentrations ranging from 0.0002 mg/mL to 1 mg/mL. The cells were then suspended and analyzed by flow cytometry to determine the amount of the fluorescence-positive cells (% gated cells) and the mean fluorescence of the cell population. Polymer uptake was time and concentration dependent (exemplarily shown for **P5**, Figure 3A and 3B) as well as temperature-dependent (Figure 3C), suggesting that endocytosis was a primary mechanism of the cellular entry.[20]

Notably, both the molar mass and structure of the polymers had major effects on the uptake. Specifically, in each pair of the homopolymers, random copolymers or block copolymers the uptake was more pronounced for a smaller polymer in the pair. Furthermore, there were striking differences in the concentration dependences of the uptake between each of the three structure types. To quantify these differences we introduced an effective concentration parameter, EC_{50}, which corresponds to the polymer concentration at which 50 % of cells were gated. It was obvious that the difference in EC_{50} of the smaller and larger homopolymers **P1** and **P2** was negligible (Figures 4A and 4B, 33 vs. 35 μM). In contrast, in the case of the random copolymers **P3** and **P4** the smaller copolymer was taken up into the cells at much lower doses than the larger copolymer (Figures 4C and 4D 0.2 vs. 15 μM). Likewise, in the case of the block copolymers **P5** and **P6** the smaller copolymer was accumulated in cells at lower doses than the larger one (Figures 4E and 4F, 7 vs. > 55 μM). We posit that observed differences in the cellular uptake of the homopolymers, random and block copolymers may be related to different mechanisms of cellular entry of the polymers with different architecture.

As shown for **P5** the cellular uptake was relatively slow and increased almost linearly as the time of incubation increased for at least 20 h (Figure 3A). Interestingly, we did not find a pronounced difference in the concentration dependent behaviour of uptake even if we incubated the cells with the polymer for 20 h. (Figure 3B). For example, in the case of **P5**, the EC_{50} after 20 h incubation was 1 μM, which was fairly close to 7 μM observed after 60 min incubation (Figure 4E). It is important to keep in mind that at the investigated concentrations the block copolymers **P5** and **P6** aggregated into micelle-like structures with a diameter of approx. 112 nm and 224 nm as reported earlier (Table 4). These structures were significantly larger than e.g. the micelles of Pluronic P85 (approx. 15 nm in diameter) that were recently shown to enter mammalian cells through a clathrin-mediated endocytosis. [20]

However, DeSimone and co-workers reported that polymer particles of 100 nm, 150 nm and even as large as several micrometers can be taken up in HeLa cells.[16] As discussed above, **P6** formed considerably larger aggregates (approx. 224 nm diameter) than those formed by **P5** (approx. 112 nm diameter). Such aggregates formed by **P6** also had a hydrophilic corona of longer HPMA chains, which likely hindered interaction of the particles with the membranes. In contrast, the aggregates formed by **P5** had considerably smaller HPMA chains, which could permit limited interactions of the particles with the cellular membranes and increased the cellular uptake.

In contrast to the block copolymers, the random copolymers **P3** and **P4** form aggregates, which are likely to be slightly more loosed and less stable than the block copolymer micelles. These structures are likely to have only small hydrophilic loops, which stabilize the aggregates' particle in aqueous solution.[45] As discussed, the loops will also contain some hydrophobic lauryl groups. Such more accessible hydrophobic groups in the corona of the aggregates can be expected to serve as anchors for unspecific adhesion to the random copolymers in cell membranes. In contrast the hydrophobic lauryl groups are not present in the corona of the block copolymer micelle.

This difference may explain why the onsets of the cellular uptake of the random copolymers were observed at very low concentrations - around 1 mg/L for **P3** (0.03 μM) and **P4** (0.1 μM). These concentrations were one to two orders of magnitude lower than in the case of the homopolymer **P1** or block copolymer **P5** that were most efficiently taken up into cells in their structure classes. Interestingly, while the onset of the uptake of the random copolymers **P3** and **P4** was observed at comparable concentrations, their concentration dependence profiles were quite distinct. Specifically, the uptake of a larger copolymer **P4** increased only slightly as the concentration increased. In contrast, the smaller copolymer **P3** exhibited a sharp increase of the uptake. As a result, the EC_{50} values for **P3** and **P4** differed by two orders of magnitude. We attribute this difference to the differences in the molar mass and sizes of the copolymer chains. As already mentioned above, we hypothesize that aggregated random copolymers can bind with the membrane via the hydrophobic anchor groups - lauryl moieties in the hydrophilic loops of the micelle. These groups are possibly more accessible than in the block copolymer micellesdue to the smaller hydrophilic corona of the random copolymer aggregates. Even though the hydrodynamic radii of both random copolymers is comparable, the cmc value of **P3** is double compared to **P4**, indicating less stable aggregates. In addition, **P3** has a higher relative amount of hydrophobic units in the polymer and therefore can be expected to have a larger number of lauryl chains in the hydrophilic loops of the aggregates. Thus, an increase in the cellular uptake of **P3** compared to **P4** is reasonable.

It is also interesting to note that while **P3** entered the cells at considerably lower concentrations than **P5**, the amount of internalized polymer increased only slowly and reached a plateau at a concentration of around 30 μM, indicating a saturation effect (Figure 4C). In contrast, **P5** uptake showed no signs of saturation resulting in greater fluorescence intensity levels than for **P3** at polymer concentrations of 1 mg/mL (Figure 4E). A laser scanning confocal microscopy study using these two polymer samples suggested a substantial difference in the sub-cellular localization of these polymers (Figure 5).

Interestingly, **P3** showed a relatively homogenous distribution within the cytosol and the nucleoplasm (Figure 5A). However, much to our surprise, more pronounced fluorescence intensity was found in the nucleoli. In contrast, the confocal micrograph of cells incubated with **P5** revealed a relatively even distribution of fluorescence throughout the cytosol, no appreciable fluorescence in the nucleoplasm and little fluorescence in the nucleoli. In both cases, however, it was clear that the polymers were not membrane bound but were taken up

into the cells and clearly were not punctuate, i.e. not restricted to vesicles within the cytosol. This is an important finding for the projected use of the HPMA-based polymers for drug delivery since it suggests that such polymers can reach various intracellular compartments.

Further investigations are necessary to understand the mechanism of endocytosis involved and the distribution of the polymeric structures within the cell. The novel synthetic approach to obtain well defined HPMA based polymers of different polymer microstructures by RAFT is important to allow the determination of these complex structure-property relationships.

Conclusion

In this work we present the synthesis of well-defined HPMA based homopolymers, random and block copolymers, which allowed us to study the structural effects on the endocytosis in MDR breast cancer cells over a wide range of concentrations. At non-toxic doses of polymers we observed that the amount of polymers taken up by the cells after 60 min of incubation strongly depended on the polymer structure and the molar mass of the samples. For HPMA homopolymers the amount of cellular uptake was relatively low while for the 15 kDa (P5) block copolymers the uptake was higher and occurred at lower concentrations. The random copolymer of 15 kDa (P3) was taken up to a similar extent. However, in contrast to a block copolymer the uptake of P3 began at lower concentrations and reached saturation at higher concentrations. We propose that the molar mass and the polymer architecture are important determinants for the endocytosis and that our new synthetic approach towards defined HPMA based copolymers allows tailoring the cellular uptake of synthetic, biocompatible polymers. More detailed investigations regarding the uptake mechanism and the suitability of these polymers for drug delivery are warranted and are currently performed in our laboratories.

Acknowledgments

References

[1]. Ferrari M. Cancer nanotechnology: opportunities and challenges. Nat Rev Cancer. 2005; 5:161–71. [PubMed: 15738981]

[2]. Ringsdorf H. Structure and properties of pharmacologically active polymers. J Polymer Sci Polym Symp. 1975; 51:135–53.

[3]. Duncan R. Polymer conjugates as anticancer nanomedicines. Nat Rev Cancer. 2006; 6:688–701. [PubMed: 16900224]

[4]. Haag R, Kratz F. Polymer Therapeutics: Concepts and Applications Angew Chem Int Ed. 2006; 45:1198–215.

[5]. Duncan R. Polymer conjugates for tumor targeting and intracytoplasmic delivery. The EPR effect as a commom gateway? Pharm Sci Technol Today. 1999; 2:441–9. [PubMed: 10542390]

[6]. Matsumura Y, Maeda H. A new concept for macromolecular therapeutics in cancer chemotherapy: mechanism of tumoritropic accumulation of proteins and the antitumor agent SMANCS. Cancer Res. 1986; 46:6387–92. [PubMed: 2946403]

[7]. Duncan R. The dawning era of polymer therapeutics. Nat. Rev. Drug Discovery. 2003; 2:347–60.

[8]. Maeda H, Wu J, Sawa Y, Matsumura Y, Hori K. Tumor vascular permeability and the EPR effect in macromolecular therapeutics: a review. J. Controlled Release. 2000; 65:271–84.

[9]. Kwon GS, Kataoka K. Block copolymer micelles as long-circulating drug vehicles. Adv Drug Delivery Rev. 1995; 16:295–309.

[10]. Harris JM, Chess RB. Effect of pegylation on pharmaceuticals. Nat Rev Drug Discovery. 2003; 2:214–21.

[11]. Greish K, Fang J, Inutsuka T, Nagamitsu A, Maeda H. Macromolecular Therapeutics: Advantages and Prospects with Special Emphasis on Solid Tumour Targeting. Clin Pharmacokinet. 2003; 42:1089–105. [PubMed: 14531722]

[12]. Lee Y, Ishii T, Cabral H, Kim HJ, Seo JH, Nishiyama N, et al. Charge-Conversional Polyionic Complex Micelles-Efficient Nanocarriers for Protein Delivery into Cytoplasm. Angew. Chem. 2009 DOI: 10.1002/ange.200900064.

[13]. Kabanov AV, Batrokova EV, Alakhov VY. Pluronic® block copolymers as novel polymer therapeutics for drug and gene delivery. J. Controlled Release. 2002; 82:189–212.

[14]. Maeda H. SMANCS and polymer-conjugated macromolecular drugs: advantages in cancer chemotherapy. Adv Drug Deliv Rev. 1991; 6:181–202.

[15]. Jiang W, Kim BYS, Rutka JT, Chan WCW. Nanoparticle-mediated cellular response is size-dependent. Nat Nanotechnol. 2008; 3:145–50. [PubMed: 18654486]

[16]. Gratton SEA, Ropp PA, Pohlhaus PD, Luft JC, Madden VJ, Napier ME, et al. The effect of particle design on cellular internalization pathways. Proc Natl Acad Sci USA. 2008; 105:11613–8. [PubMed: 18697944]

[17]. Gratton SEA, Napier ME, Ropp PA, Tian S, DeSimone JM. Microfabricated Particles for Engineered Drug Therapies: Elucidation into the Mechanisms of Cellular Internalization of PRINT Particles. Pharm Res. 2008; 25:2845–52. [PubMed: 18592353]

[18]. Verma A, Uzun O, Hu Y, Hu Y, Han HS, Watson N, et al. Surface-structure-regulated cell-membrane penetration by monolayer-protected nanoparticles. Nat Mater. 2008; 7:588–95. [PubMed: 18500347]

[19]. Batrakova EV, Li S, Alakhov VY, Miller DW, Kabanov AV. Optimal Structure Requirements for Pluronic Block Copolymers in Modifying P-glycoprotein Drug Efflux Transporter Activity in Bovine Brain Microvessel Endothelial Cells. J Pharmacol Exp Ther. 2003; 304:845–54. [PubMed: 12538842]

[20]. Sahay G, Batrakova EV, Kabanov AV. Different Internalization Pathways of Polymeric Micelles and Unimers and Their Effects on Vesicular Transport. Bioconjugate Chem. 2008; 19:2023–29.

[21]. Kissel M, Peschke P, Šubr V, Ulbrich K, Schuhmacher J, Debus J, et al. Synthetic macromolecular drug carriers: biodistribution of poly[(N-2-hydroxypropyl)methacrylamide] and its accumulation in solid rat tumors. PDA J Pharm Sci Tech. 2001; 55:191–201.

[22]. Duncan R, Cable HC, Lloyd JB, Rejmanová P, Kopecek J. Polymers containing enzymatically degradable bonds, 7. Design of oligopeptide side-chains in poly[N-(2-hydroxypropyl)methacrylamide] copolymers to promote efficient degradation by lysosomal enzymes. Makromol Chem. 1983; 184:1997–2008.

[23]. Kopecek J, Kopeková P, Minko T, Lu ZR. HPMA copolymer-anticancer drug conjugates: design, activity, and mechanism of action. Eur J Pharm Biopharm. 2000; 50:61–81. [PubMed: 10840193]

[24]. Vicent MJ, Greco F, Nicholson RI, Paul A, Griffiths PC, Duncan R. Polymer Therapeutics Designed for a Combination Therapy of Hormone-Dependent Cancer. Angew Chem Int Ed. 2005; 44:4061–66.

[25]. Konak C, Matyjaszewski K, Kopeckova P, Kopecek J. Poly[N-(2-hydroxypropyl)methacrylamide-block-n-butyl acrylate] micelles in water/DMF mixed solvents. Polymer. 2002; 43:3735–41.

[26]. Barz M, Tarantola M, Fischer K, Schmidt M, Luxenhofer R, Janshoff A, et al. From Defined Reactive Diblock Copolymers to Functional HPMA-Based Self-Assembled Nanoaggregates. Biomacromolecules. 2008; 9:3114–18. [PubMed: 18855476]

[27]. Herth M, Barz M, Moderegger D, Allmeroth M, Jahn M, Thews O, et al. Radioactive Labeling of Defined HPMA-Based Polymeric Structures Using [18F]FETos for In Vivo Imaging by Positron Emission Tomography. Biomacromolecules. 2009 accepted.

[28]. Matyjaszewski K, Xia J. Atom Transfer Radical Polymerization. Chem Rev. 2001; 101:2921–90. [PubMed: 11749397]

[29]. Matyjaszewski, K.; Gnanou, Y.; Leibler, L. Macromolecular Engineering. Vol. 1. Wiley-VCH; Weinheim: 2007.

[30]. Tsarevsky NV, Matyjaszewski K. "Green" Atom Transfer Radical Polymerization: From Process Design to Preparation of Well-Defined Environmentally Friendly Polymeric Materials. Chem Rev. 2007; 107:2270–99. [PubMed: 17530906]

[31]. Barner-Kowollik, C. Handbook of RAFT Polymerization. Wiley-VCH; Germany; Weinheim: 2008.

[32]. Moad G, Rizzardo E, Thang SH. Living Radical Polymerization by the RAFT Process. Aust J Chem. 2005; 58:379–410.

[33]. Moad G, Rizzardo E, Thang SH. Radical addition–fragmentation chemistry in polymer synthesis. Polymer. 2008; 49:1079–131.

[34]. Batz HG, Franzmann G, Ringsdorf H. Model Reactions for Synthesis of Pharmacologically Active Polymers by Way of Monomeric and Polymeric Reactive Esters. Angew Chem Int Ed. 1972; 11:1103–04.

[35]. Ferruti A, Bettelli A, Fere A. High polymers of acrylic and methacrylic esters of N-hydroxysuccinimide as polyacrylamide and polymethacrylamide precursors. Polymer. 1972; 13:462–4.

[36]. Eberhardt M, Mruk R, Zentel R, Theato P. New precursor polymers for the synthesis of multifunctional materials. Eur Polym J. 2005; 41:1569–75.

[37]. Theato P. Synthesis of well-defined polymeric activated esters. J Polym Sci Part A: Polym Chem. 2008; 46:6677–87.

[38]. Perrier S, Takolpuckdee P, Mars CA. Reversible Addition-Fragmentation Chain Transfer Polymerization: End Group Modification for Functionalized Polymers and Chain Transfer Agent Recovery. Macromolecules. 2005; 38:2033–6.

[39]. Colombani O, Ruppel M, Schubert F, Zettl H, Pergushov DV, Müller AHE. Synthesis of Poly(n-butyl acrylate)-block-poly(acrylic acid) Diblock Copolymers by ATRP and Their Micellization in Water. Macromolecules. 2007; 40:4338–50.

[40]. Wilhelm M, Zhao CL, Wang Y, Xu R, Winnik MA, Mura JL, et al. Poly(styrene-ethylene oxide) block copolymer micelle formation in water: a fluorescence probe study. Macromolecules. 1991; 24:1033–40.

[41]. Kalyanasundaram K, Thomas JK. Environmental effects on vibronic band intensities in pyrene monomer fluorescence and their application in studies of micellar systems. J Am Chem Soc. 1977; 99:2039–44.

[42]. Borisov OV, Halperin A. Extending polysoaps in the presence of free amphiphiles. Physical Review E. 1998; 57:812–22.

[43]. Liu RCW, Pallier A, Brestaz M, Pantoustier N, Tribet C. Impact of Polymer Microstructure on the Self-Assembly of Amphiphilic Polymers in Aqueous Solutions. Macromolecules. 2007; 40:4276–86.

[44]. Noda T, Hashidzume A, Morishima Y. Micelle Formation of Random Copolymers of Sodium 2-(Acrylamido)-2-methylpropanesulfonate and a Nonionic Surfactant Macromonomer in Water As Studied by Fluorescence and Dynamic Light Scattering. Macromolecules. 2000; 33:3694–704.

[45]. Borisov OV, Halperin A. Micelles of Polysoaps: The Role of Bridging Interactions. Macromolecules. 1996; 29:2612–7.

[46]. Herzlinger DA, Easton TG, Ojakian GK. The MDCK epithelial cell line expresses a cell surface antigen of the kidney distal tubule. J Cell Biol. 1982; 93:269–77. [PubMed: 6178742]
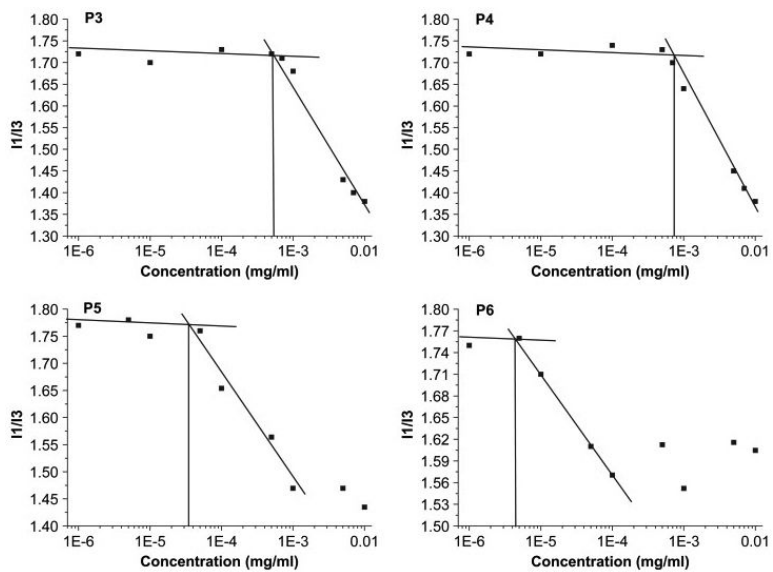
Figure 1.
The cmc estimation of random copolymer **P3**, **P4** and block copolymer **P5**, **P6** by pyrene fluorescence spectroscopy in isotonic solution at pH 7
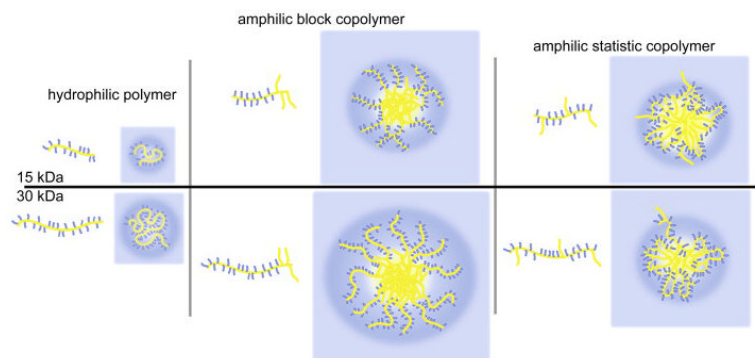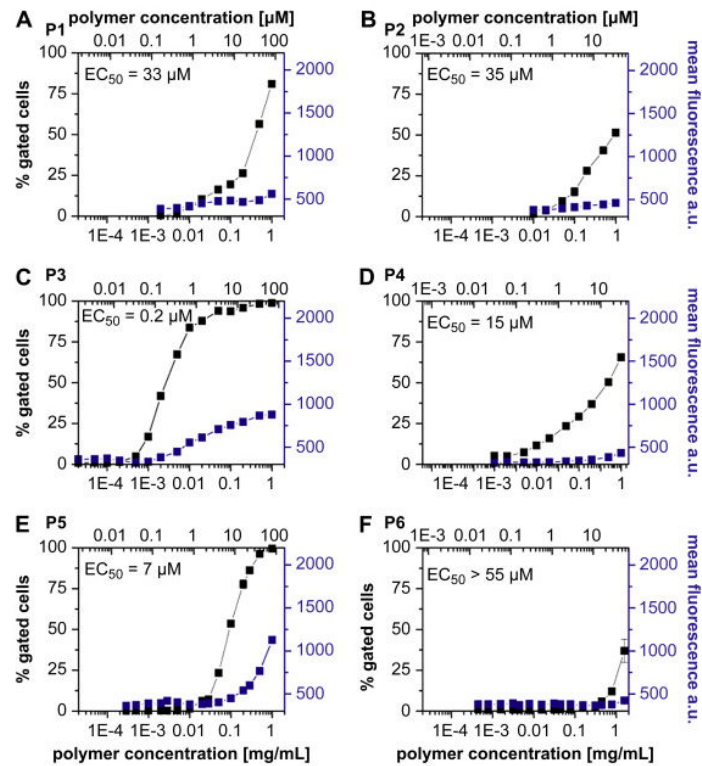
Figure 2.
Schematic sketch of self-assembled polymeric structures in aqueous solution (blue parts: hydrophilic, yellow parts: hydrophobic). Homopolymers are present as unimers (left), block copolymers from polymer micelles or micelle like core-shell aggregates (center) while random copolymers can form less stable aggregates through intra- and interchain interactions.
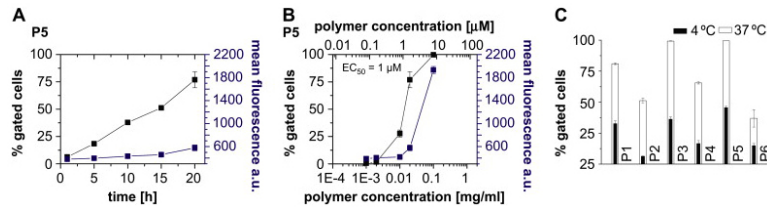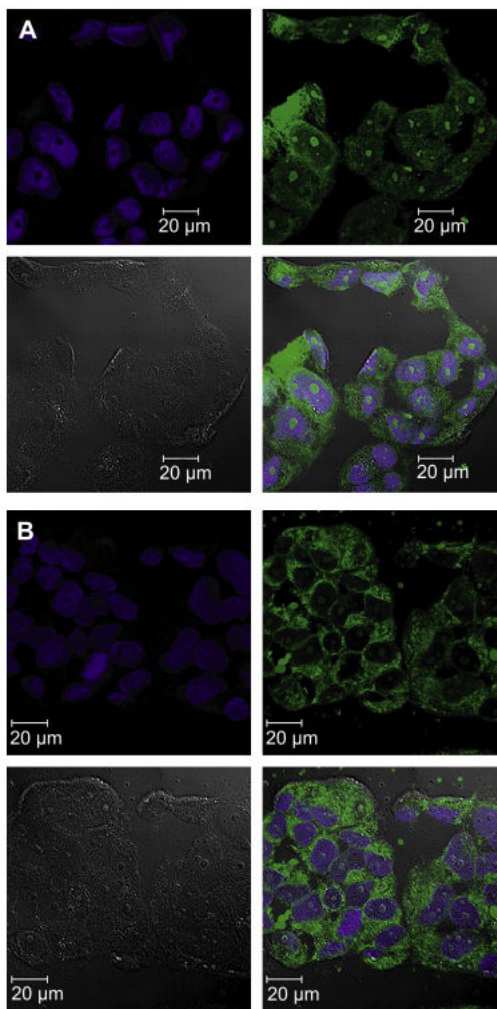
Figure 3.
Time (A), concentration (B, 20h incubation) and temperature (C) dependence of cellular uptake of **P5** (A and B) and **P1**-**P6** (C), respectively, as obtained from flow cytometry (% gated cells left; ■ and mean fluorescence per gated event right; ▪). EC50 value shows the concentration where 50 % gated cells are observed and were obtained by graphical extraction. Data is represented as mean ± SEM (n=3).

Figure 4.
Concentration dependent endocytosis of fluorescently labelled polymer samples **P1**-**P6** (A-D). MCF7/ADR cells were incubated for 60 min at 37°C and subsequently analyzed by flow cytometry. In each diagram, the concentration (upper x-axis molar concentration; lower x-axis mass concentration β, is plotted against % gated cells (left, ■) and mean fluorescence per gated event (right, ■). EC_{50} values show the concentration where 50 % gated cells are observed and were obtained by graphical extraction. Data is represented as mean ± SEM (n=3).
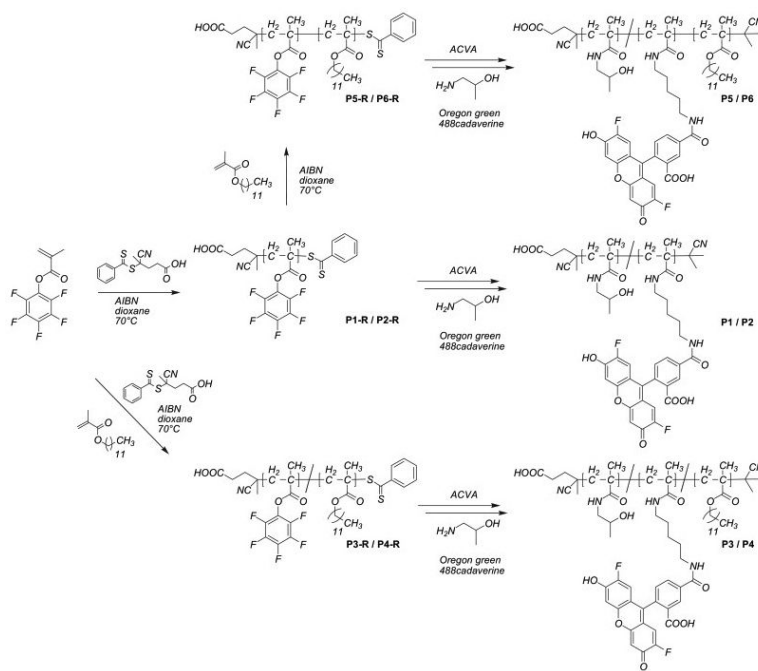
Figure 5.
Confocal microscopy images taken from live MCF7/ADR cells after incubation with 1 mg/ mL **P3** (A) or **P5** (B) for 60 min. Nuclei were stained using DRAQ5 (Biostatus Limited, UK), polymers were labelled with oregon green 488. Pictures showing from top left to bottom right DRAQ5, polymer, DIC and merge respectively.

Scheme 1.
Synthetic pathway to fluorescently labelled homopolymers, random copolymers and block copolymers based on pHPMA using the active ester approach.

Table 1

Characteristics of reactive homopolymers (**P1R, P2R**), copolymers (**P3R, P4R**) and block copolymers (**P5R, P6R**)

	structure	monomer ratio [a]	M_n [b]	M_w [b]	PDI [b]
P1R	homopolymer	100:0	21.1	25.1	1.19
P2R	homopolymer	100:0	50.2	60.8	1.21
P3R	random copolymer	80:20	22.3	27.4	1.23
P4R	random copolymer	80:20	50.0	59.8	1.20
P5R	block copolymer	80:20	24.7	28.6	1.20
P6R	block copolymer	90:10	52.2	65.8	1.26

[a] Calculated monomer ratio

[b] kg/mol, determined by GPC in THF as solvent for the activated ester polymers P1R to P6R

NIH-PA Author Manuscript

NIH-PA Author Manuscript

NIH-PA Author Manuscript

Table 2

Characteristics of HPMA based random copolymers (**P1,P2,P3,P4**) and block copolymers (**P5,P6**).

	structure	HPMA/LMAunit ratio [a]	M_n [b]	M_w [b]	PDI [b]
P1	homopolymer	100:0	12.2	14.3	1.19
P2	homopolymer	100:0	28.7	40.0	1.21
P3	random copolymer	78:22	14.6	20.2	1.23
P4	random copolymer	81:19	32.8	39.3	1.20
P5	block copolymer	79:21	12.5	15.4	1.20
P6	block copolymer	88:12	27.7	32.5	1.26

[a] As determined by ^{1}H NMR spectroscopy after aminolysis with hydroxypropylamine yielding **P1** to **P6**

[b] kg/mol, determined by GPC in THF as solvent for the activated ester polymers **P1R** to **P6R**.

Table 3

The cmc of the block copolymers (**P3-P6**) in isotonic solution

	Structure	Cmc	
		mg/mL[a]	mol/L[a]
P3	random copolymer	5.3×10^{-4}	3.6×10^{-8}
P4	random copolymer	7.2×10^{-4}	2.2×10^{-8}
P5	block copolymer	2.4×10^{-5}	1.9×10^{-9}
P6	block copolymer	4.1×10^{-6}	1.5×10^{-10}

[a]As determined by pyrene fluorescence spectroscopy

Table 4

Characterization of aggregates from **P3** to **P6** in hexafluoroisopropanol (HFIP) and aqueous NaBr (1×10^{-3} M) solution

	R_h (nm) in HFIP	c (mg/mL) in aqueous solution	R_h (nm) in aqueous solution	μ_2
P3	3.1 ± 0.15	0.01	37.2	0.11
P4	3.8 ± 0.15	0.01	32.3	0.09
P5	3.0 ± 0.15	0.01	55.7	0.08
P6	3.8 ± 0.15	0.01	112	0.07